MÁRTA SZILVÁSI-NAGY
TERÉZ P. VENDEL
HELLMUTH STACHEL

C^2 Filling of Gaps by Convex Combination of Surfaces under Boundary Constraints

C^2 popunjavanje praznina pomoću konveksne kombinacije ploha pod rubnim ograničenjima

SAŽETAK

Dane su dvije metode za izvođenje ploha. Jedna za povezivanje dviju ploha sa C^2 neprekinutošću koja odgovara i dvjema graničnim linijama, a druga za G^1 popunjavanje posebnog slučaja trostrane rupe. Plohe se izvode kao konveksna kombinacija plošnih i krivuljnih sastvanih dijelova sa odgovarajućom korektivnom funkcijom, a dane su u parametarskom obliku.

Ključne riječi: C^2 neprekinutost, konveksna kombinacija, Coonsove plohe, popunjavanje rupa, plošno modeliranje

C^2 Filling of Gaps by Convex Combination of Surfaces under Boundary Constraints

ABSTRACT

Two surface generation methods are presented, one for connecting two surfaces with C^2 continuity while matching also two prescribed border lines on the free sides of the gap, and one for G^1 filling a three-sided hole in a special case. The surfaces are generated as convex combination of surface and curve constituents with an appropriate correction function, and are represented in parametric form.

Key words: C^2 continuity, Convex combination, Coons surfaces, Filling of holes, Surface modelling

MSC 2000: 65D17, 68U07

1 Introduction

In this paper trigonometric convex combinations of surfaces and curves are applied for filling gaps between two surfaces and holes bounded by three surfaces. Trigonometric blending functions have been applied for G^1 curve construction already by Bär (1977), then for defining G^2 spline curves as convex combinations of arcs and straight line segments by Szilvási-Nagy and P.Vendel (2000). An extension of those curve constructions to surfaces has been given by Szilvási-Nagy (2000). Continuity conditions and a rational parametric form of the blending functions are presented here.

Convex combinations of points, curves or surfaces are frequently used for solving interpolation problems, for example Little (1983). Well-known interpolating surfaces defined by convex combination of boundary curves are the Coons surfaces (see e.g. in Farin 1990). Curves defined over triangles are interpolated by a C^2 surface using quintic polynomials by Alfeld and Barnhill (1984). Here, similarly to Coons's method, the input data are "wire frame data" consisting of curves and first and second cross-boundary derivatives. A transfinite blending function interpolant for the simplex in $\mathbf{R}^n$ is decribed by Gregory (1985). The term transfinite means that the interpolant matches function and derivative values given on all faces of the simplex. That is, surfaces appear in the combination. The method is based on an explicit representation of a finite dimensional Hermite interpolation polynomial for the simplex.

The surface generation methods presented in this paper formally follow the construction method of Coons by building a convex combination of the boundary data and applying proper correction functions. However, the geometric concept of our construction is rather similar to the transfinite interpolation surface of Gregory. The use of surface patches in a Coons-type blend is novel in our algorithms. The surfaces in the combination are defined over the same parameter domain. The resulting surface matches one bordering line of each surface and the tangent planes along this line. Moreover, the second cross-derivatives are also equal along the contact curves in the rectangular case (first algorithm). This fact can be used for filling a gap between two surfaces or a hole between three surfaces. The constituents are either the extensions of the surfaces bordering

the gap or the hole, or patches (two or three) joining C^1 or C^2 continuously to one of the surfaces which are to be connected. In this way these patches transfer the boundary data to the convex combination. There are several known methods for C^1 or C^2 fitting of rectangular and triangular patches (Farin, 1990, Chapter 19 and Hoschek, 1992, Chapter 7). These constructions will not be the subject of this paper.

2 Blending surface between two surfaces with boundary constraints

A blending surface is one that smoothly connects two given surfaces and satisfies additional geometric constraints. Filip (1989) applied cubic Hermite blend of two boundary curves of the given surfaces and two arbitrary rail curves. The literature describes many different methods for constructing blending surfaces, recently Hartmann (2001) used rational functions. Some of these methods are extended to three or more surfaces, for example that of Schichtel (1993). These blending surfaces defined as linear combinations of given curves or surfaces with one parameter blending functions are different from both the Coons and our patches, they are not the subject of this paper.

In this algorithm two regular surfaces $\mathbf{r}_1(u,v)$ and $\mathbf{r}_2(u,v)$ and two curves $\mathbf{r}_3(v)$ and $\mathbf{r}_4(v)$ are given. The curves join the corresponding corner points of the two surfaces as boundary lines of the required surface patch. The blending surface is defined over the parameter domain $(u,v) \in [0,1] \times [0,1]$ such that its boundary curves for $v = 0$ and $v = 1$ match the boundaries of the gap determined from the left by $\mathbf{r}_1(u,0)$ and from the right by $\mathbf{r}_2(u,1)$, respectively, while the upper border line for $u = 0$ coincides with the curve $\mathbf{r}_3(v)$ and the lower border line for $u = 1$ coincides with the curve $\mathbf{r}_4(v)$ ($v \in [0,1]$) (Fig. 1). The drawn parts of the given underlying surfaces in Fig. 2 are parametrized as follows: $\mathbf{r}_1(u,v)$: $(u,v) \in [0,1] \times [-1,0]$, and $\mathbf{r}_2(u,v)$: $(u,v) \in [0,1] \times [1,2]$.
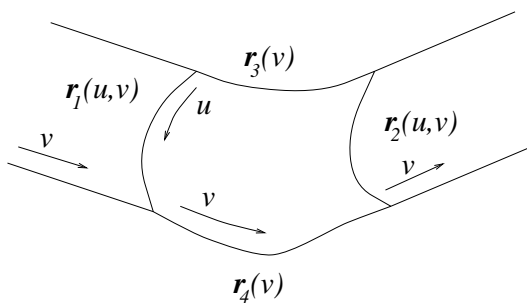
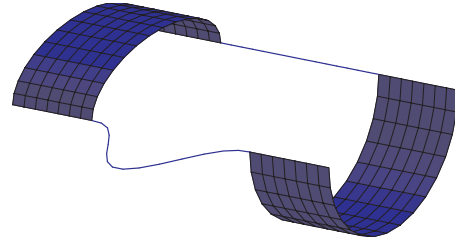

Figure 1: Two surfaces and two curves bordering a gap.

Figure 2: The input surfaces and curves determining a gap.

The blending surface $\mathbf{f}(u,v)$ is generated by a trigonometric convex combination of the surfaces and curves and by an appropriate correction function (Fig. 3).
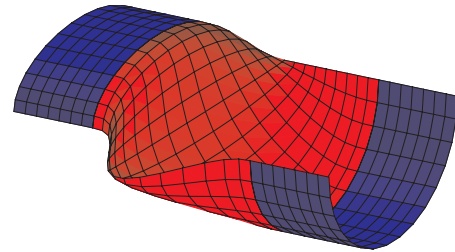

Figure 3: The filled gap shown in Fig. 2.

Theorem 1 *Let two surfaces be given by the differentiable vector functions* $\mathbf{r}_1(u,v)$ *and* $\mathbf{r}_2(u,v)$ *over a parameter domain containing the unit square* $[0,1] \times [0,1]$ *moreover, two curve segments given by the differentiable vector functions* $\mathbf{r}_3(v)$ *and* $\mathbf{r}_4(v)$, $v \in [0,1]$. *In the corner points*

$$\mathbf{r}_1(0,0) = \mathbf{r}_3(0), \quad \mathbf{r}_1(1,0) = \mathbf{r}_4(0),$$
$$\mathbf{r}_2(0,1) = \mathbf{r}_3(1), \quad \mathbf{r}_2(1,1) = \mathbf{r}_4(1)$$

are required.
Then the surface defined by the following vector equation

$$
\begin{aligned}
\mathbf{f}(u,v) = {} & \cos^2(\frac{\pi}{2} \cdot v)\mathbf{r}_1(u,v) + \sin^2(\frac{\pi}{2} \cdot v)\mathbf{r}_2(u,v) \\
& + \cos^2(\frac{\pi}{2} \cdot u)\mathbf{r}_3(v) + \sin^2(\frac{\pi}{2} \cdot u)\mathbf{r}_4(v) \\
& - \mathbf{q}(u,v),
\end{aligned}
\tag{1}
$$

where $\quad \mathbf{q}(u,v) = [\cos^2(\frac{\pi}{2} \cdot v)\mathbf{r}_1(0,v)$

$\qquad\qquad + \sin^2(\frac{\pi}{2} \cdot v)\mathbf{r}_2(0,v)]\cos^2(\frac{\pi}{2} \cdot u)$

$\qquad\qquad + [\cos^2(\frac{\pi}{2} \cdot v)\mathbf{r}_1(1,v)$

$\qquad\qquad + \sin^2(\frac{\pi}{2} \cdot v)\mathbf{r}_2(1,v)]\sin^2(\frac{\pi}{2} \cdot u),$

and $\quad (u,v) \in [0,1] \times [0,1],$

is differentiable and fits the boundary curves $\mathbf{r}_1(u,0)$, $\mathbf{r}_2(u,1)$, $\mathbf{r}_3(v)$ *and* $\mathbf{r}_4(v)$.

Proof. The border lines of the patch $\mathbf{f}(u,v)$ are to be checked by substituting $u = 0$, $u = 1$, $v = 0$, and $v = 1$ into the equation (1) in turn. The computation results with $\mathbf{f}(0,v) = \mathbf{r}_3(v)$, $\mathbf{f}(1,v) = \mathbf{r}_4(v)$, $\mathbf{f}(u,0) = \mathbf{r}_1(u,0)$, $\mathbf{f}(u,1) = \mathbf{r}_2(u,1)$, $u \in [0,1]$, $v \in [0,1]$ as stated in the Theorem. ⋄

Theorem 2 *The surface defined in (1) joins to the given surface $\mathbf{r}_1(u,v)$ with first order (C^1) continuity along the boundary line $\mathbf{r}_1(u,0)$, $u \in [0,1]$, when the curves $\mathbf{r}_3(v)$ and $\mathbf{r}_4(v)$ join with C^1 continuity to the border lines $u = 0$ and $u = 1$ of the surface $\mathbf{r}_1(u,v)$, respectively.*

Proof. According to the conditions $\mathbf{r}_{1,v}(0,0) = \mathbf{r}_{3,v}(0)$ and $\mathbf{r}_{1,v}(1,0) = \mathbf{r}_{4,v}(0)$, where the subscript v denotes the differentiation with respect to v. According to Theorem 1 $\mathbf{f}(u,0) = \mathbf{r}_1(u,0)$, therefore the partial derivatives $\mathbf{f}_u(u,0)$ and $\mathbf{r}_{1,u}(u,0)$ are equal along the common boundary curve $v = 0$, $u \in [0,1]$. The tangent vector of a v parameter line of the surface $\mathbf{f}(u,v)$ at a point of this curve is

$$\begin{aligned} \mathbf{f}_v(u,0) &= \mathbf{r}_{1,v}(u,0) + \cos^2(\frac{\pi}{2} \cdot u)(\mathbf{r}_{3,v}(0) - \mathbf{r}_{1,v}(0,0)) \\ &+ \sin^2(\frac{\pi}{2} \cdot u)(\mathbf{r}_{4,v}(0) - \mathbf{r}_{1,v}(1,0)). \end{aligned}$$

By assumption, the second and third terms are zero vectors, consequently $\mathbf{f}_v(u,0) = \mathbf{r}_{1,v}(u,0)$ at the points of the connection line. This means C^1 continuity between $\mathbf{f}(u,v)$ and $\mathbf{r}_1(u,v)$ at the points $v = 0$, $u \in [0,1]$. Therefore, the tangent planes of the two surfaces along the connection line are obviously the same. ⋄

Remark 1. The analogous statement about the C^1 connection of the blending surface $\mathbf{f}(u,v)$ defined in (1) and $\mathbf{r}_2(u,v)$ along the connection line $v = 1$ yields if $\mathbf{r}_3(v)$ and $\mathbf{r}_4(v)$ join with C^1 continuity to the border lines $u = 0$ and $u = 1$ of $\mathbf{r}_2(u,v)$, respectively. The proof is similar to that of Theorem 2.

Remark 2. In the case if $\mathbf{r}_1(u,v)$ (and analogously $\mathbf{r}_2(u,v)$) is a cylindrical surface, G^1 continuous connection between $\mathbf{r}_1(u,v)$ (or $\mathbf{r}_2(u,v)$) and $\mathbf{f}(u,v)$ can be assured under weaker conditions, namely, when $\mathbf{r}_{3,v}(0)$ is parallel to $\mathbf{r}_{1,v}(0,0)$ and $\mathbf{r}_{4,v}(0)$ is parallel to $\mathbf{r}_{1,v}(1,0)$ (G^1 condition instead of C^1). As the derivatives with respect to v of the cylindrical surface $\mathbf{r}_1(u,v)$ (see Fig. 4) are all parallel, the terms in the expression of $\mathbf{f}_v(u,0)$ are parallel to $\mathbf{r}_{1,v}(u,0)$, which ensures the parallelity of the normals $\mathbf{f}_u(u,0) \times \mathbf{f}_v(u,0)$ and $\mathbf{r}_{1,u}(u,0) \times \mathbf{r}_{1,v}(u,0)$.
The tangent plane continuity is equivalent to the G^1 continuity. In this case the joining surface patches admit a local reparametrisation in which the joining surfaces are C^1 (Boehm, 1988 and Gregory, 1989).

The conditions in Remark 2 allow flexible constructions of blending surfaces between cylindrical surfaces. In the next example the upper and lower curves connect the border lines of the two cylindrical surfaces with G^1 continuity. The convex combination surface generated in the rational parametric form of the trigonometric blendig functions (see in Section 4.) fits the prescribed boundary curves and joins with tangential continuity (G^1) to the two cylindrical surfaces (Fig. 4.). Similar modelling problems occur e.g. in planning canals over a landscape by joining cylindrical or toroidal surfaces while also matching prescribed bordering curves.
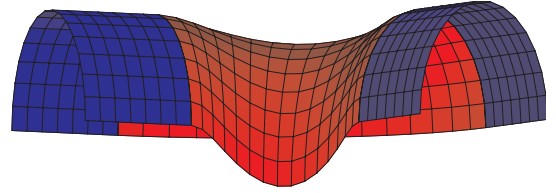

Figure 4: G^1 continuous input data result G^1 connection.

Theorem 3 *If the boundary curves $\mathbf{r}_3(v)$ and $\mathbf{r}_4(v)$ join C^2 continuously to the boundary lines $u = 0$ and $u = 1$ of the surfaces $\mathbf{r}_1(u,v)$ and $\mathbf{r}_2(u,v)$ at the corner points, then adding the correction function*

$$\begin{aligned} \mathbf{m}(u,v) &= s(v) \cdot [\mathbf{r}_1(u,v) - \mathbf{r}_2(u,v) \\ &- \cos^2(\frac{\pi}{2} \cdot u)(\mathbf{r}_1(0,v) - \mathbf{r}_2(0,v)) \\ &- \sin^2(\frac{\pi}{2} \cdot u)(\mathbf{r}_1(1,v) - \mathbf{r}_2(1,v))] \end{aligned}$$

to the expression of $\mathbf{f}(u,v)$ in (1), where

$$s(v) = \frac{1}{16}(-2v+1)^3 \sin^2(\pi(2v+1))$$

results C^2 connection of $\mathbf{f}(u,v)$ with $\mathbf{r}_1(u,v)$ and $\mathbf{r}_2(u,v)$.

Proof. The requirements of Theorem 2 are obviously fullfilled for both surfaces $\mathbf{r}_1(u,v)$ and $\mathbf{r}_2(u,v)$. As the values of $s(v)$ and $s'(v)$ at $v = 0$ and $v = 1$ are zero, the new term $\mathbf{m}(u,v)$ in (1) does not influence the C^0 and C^1 continuities. The second derivatives are $s_{vv}(0) = 1$ and $s_{vv}(1) = -1$ therefore, the differences $\mathbf{f}_{vv}(u,0) - \mathbf{r}_{1,vv}(u,0)$ and $\mathbf{f}_{vv}(u,1) - \mathbf{r}_{2,vv}(u,1)$ become zero. ⋄

C^2 continuous filling of a gap is shown in Fig. 5. This example shows also the shape influence of the underlying surfaces, where the surface $\mathbf{r}_1(u,v)$ has periodic bulges and $\mathbf{r}_2(u,v)$ is planar. The resulting surface is the combination of such a bulge and a planar rectangle and two bordering straight line segments.
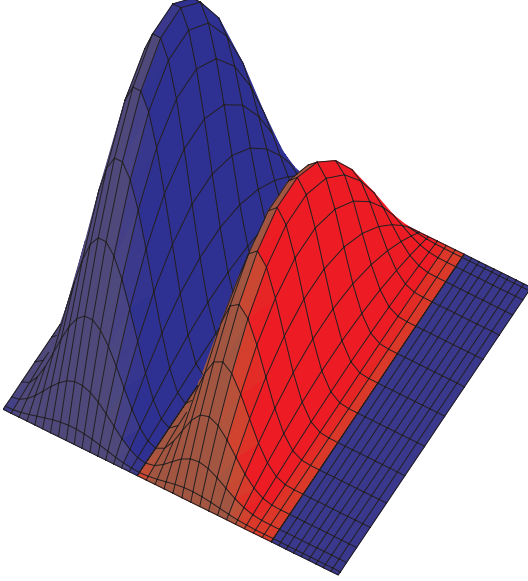
Figure 5: Shape influence of the constituents, C^2 connection.

Several experiments have shown that monoton polynomial parameter transformations of the underlying surfaces in v direction have no noticeable influence on the shape of the resulting surface.

3 Combination of three surfaces

The two parameter representation of the sphere has inspired the following trigonometric convex combination of three surfaces defined over the unit square $(u,v) \in [01,] \times [0,1]$.

Theorem 4 *If three surfaces represented by the differentiable vector functions* $\mathbf{r}_1(u,v)$, $\mathbf{r}_2(u,v)$ *and* $\mathbf{r}_3(u,v)$ *over the unit square* $(u,v) \in [0,1] \times [0,1]$ *have common corner points at* $(u,v) = (1,0)$ *and* $(u,v) = (1,1)$, *then the surface described by the vector function*

$$
\begin{aligned}
\mathbf{f}(u,v) &= \cos^2(\frac{\pi}{2} \cdot u)\cos^2(\frac{\pi}{2} \cdot v)\mathbf{r}_1(u,v) \\
&+ \cos^2(\frac{\pi}{2} \cdot u)\sin^2(\frac{\pi}{2} \cdot v)\mathbf{r}_2(u,v) \\
&+ \sin^2(\frac{\pi}{2} \cdot u)\mathbf{r}_3(u,v) - \mathbf{q}(u,v), \quad (2)
\end{aligned}
$$

where

$$
\begin{aligned}
\mathbf{q}(u,v) &= \sin^2(\frac{\pi}{2} \cdot u)\cos^2(\frac{\pi}{2} \cdot v)[\mathbf{r}_3(u,0) - \mathbf{r}_1(u,0)] \\
&+ \sin^2(\frac{\pi}{2} \cdot u)\sin^2(\frac{\pi}{2} \cdot v)[\mathbf{r}_3(u,1) - \mathbf{r}_2(u,1)]
\end{aligned}
$$

and $(u,v) \in [0,1] \times [0,1]$

is differentiable and fits the boundary curves $\mathbf{r}_1(u,0)$, $\mathbf{r}_2(u,1)$ *and* $\mathbf{r}_3(1,v)$.

Proof. The boundary lines of the blending surface $\mathbf{f}(u,v)$ are to be computed by substituting the parameter values according to the bordering lines of the unit square in the u,v parameter plane in turn.

$$
\begin{aligned}
\mathbf{f}(1,v) &= \mathbf{r}_3(1,v) - \cos^2(\frac{\pi}{2} \cdot v)[\mathbf{r}_3(1,0) - \mathbf{r}_1(1,0)] \\
&- \sin^2(\frac{\pi}{2} \cdot v)[\mathbf{r}_3(1,1) - \mathbf{r}_2(1,1)] = \mathbf{r}_3(1,v), \\
\mathbf{f}(u,0) &= \cos^2(\frac{\pi}{2} \cdot u)\mathbf{r}_1(u,0) + \sin^2(\frac{\pi}{2} \cdot u)\mathbf{r}_3(u,0) \\
&- \sin^2(\frac{\pi}{2} \cdot u)[\mathbf{r}_3(u,0) - \mathbf{r}_1(u,0)] = \mathbf{r}_1(u,0), \\
\mathbf{f}(u,1) &= \cos^2(\frac{\pi}{2} \cdot u)\mathbf{r}_2(u,1) + \sin^2(\frac{\pi}{2} \cdot u)\mathbf{r}_3(u,1) \\
&- \sin^2(\frac{\pi}{2} \cdot u)[\mathbf{r}_3(u,1) - \mathbf{r}_2(u,1)] = \mathbf{r}_2(u,1),
\end{aligned}
$$

since the corner points standing in the same brackets are equal. $\diamond$

In Fig. 6 Three cylindrical surfaces are given obeying the conditions of Theorem 4. The drawn pieces are in turn $\mathbf{r}_1(u,v)$: $(u,v) \in [0,1] \times [-1,0]$, $\mathbf{r}_2(u,v)$: $(u,v) \in [0,1] \times [1,2]$ and $\mathbf{r}_3(u,v)$: $(u,v) \in [1,2] \times [0,1]$. The generated surface patch joins continuously to the three neighbours along their boundary curves.
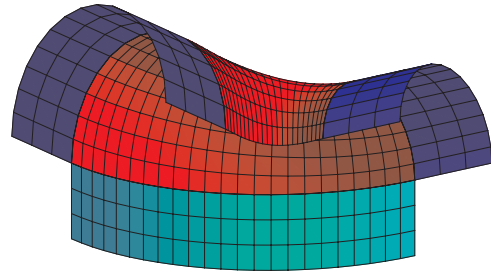

Figure 6: Combination of three surfaces, G^1 connection

The filling of a three-sided hole with a surface joining continuously to the surrounding surfaces is a classical problem, the so called suit case corner problem. The method presented here also gives a solution for this problem in a special case. The restriction in the algorithm is that two of the patches in the convex combination are three-sided degenerate surfaces meeting with their singular points at a corner of the hole. These are e.g. parts of two different rotational surfaces represented as degenerate rectangular patches (this is usually the case in CAD systems), or triangular patches, each joining with G^1 continuity to one bordering surface, then reparametrized. Such a reparametrization of a triangular domain described by the barycentric coordinates $0 \le u,v,w \le 1$, $u+v+w = 1$, is given by $u = t - s \cdot t$, $v = s \cdot t$, $0 \le s,t \le 1$.

The surface generated by equation (2) fills the three-sided hole. It is a degenerate rectangular patch, where the boundary line $u = 0$ is just a point, i.e. one corner point of the triangular hole. Surfaces with singular points (e.g. cones) are also allowed in the construction, therefore nothing can be stated about the tangent plane at the singular point in general.
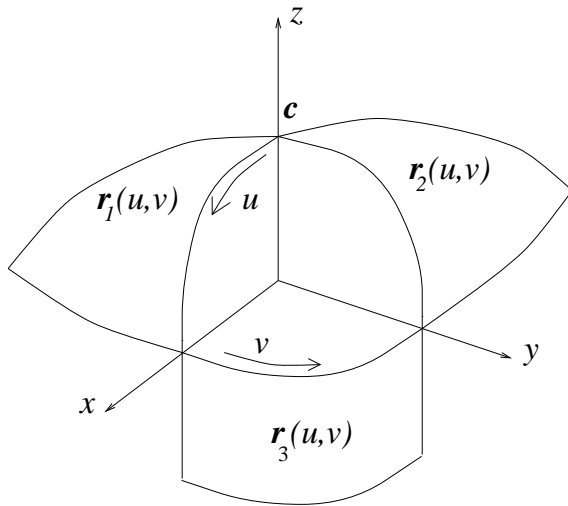

Figure 7: Three-sided hole formed by three surfaces.

In Fig. 7 a sketch of three surfaces is shown.

Theorem 5 *Let three surfaces be given by the differentiable vector functions* $\mathbf{r}_1(u,v)$, $\mathbf{r}_2(u,v)$ *and* $\mathbf{r}_3(u,v)$ *over a parameter domain containing the unit square* $[0,1] \times [0,1]$ *such that* $\mathbf{r}_1(0,v) = \mathbf{r}_2(0,v) = \mathbf{c}$, $\mathbf{r}_1(1,0) = \mathbf{r}_3(1,0)$ *and* $\mathbf{r}_2(1,1) = \mathbf{r}_3(1,1)$ *hold. Then the surface described by the vector function (2) is differentiable and fits the boundary curves* $\mathbf{r}_1(u,0)$, $\mathbf{r}_2(u,1)$ *and* $\mathbf{r}_3(1,v)$.

Proof. The equation of the boundary line $u = 0$ is

$$\mathbf{f}(0,v) = \cos^2(\frac{\pi}{2} \cdot v) \cdot \mathbf{r}_1(0,v) + \sin^2(\frac{\pi}{2} \cdot v) \cdot \mathbf{r}_2(0,v).$$

Hence the corner points are

$$\mathbf{f}(0,0) = \mathbf{r}_1(0,0), \quad \mathbf{f}(0,1) = \mathbf{r}_2(0,1).$$

The parameter line $u = 0$ collapses into a point only in the case when $\mathbf{r}_1(0,v)$ and $\mathbf{r}_2(0,v)$, $v \in [0,1]$ collapse also into the same point $\mathbf{c}$. The other three boundary curves are as in Theorem 4. ◇

Corollary 1 *If the surfaces surrounding the hole are parts of the same sphere in the same parametrization, then the surface defined in (2) is also lying on this sphere.*

Theorem 6 *If for the given three surfaces the conditions of Theorem 5, moreover the following parallelity conditions*

$$\mathbf{r}_{1,v}(u,0) \,||\, \mathbf{r}_{3,v}(u,0) \quad \mathbf{r}_{2,v}(u,1) \,||\, \mathbf{r}_{3,v}(u,1),$$

and the equalities

$$\mathbf{r}_{1,u}(1,0) = \mathbf{r}_{3,u}(1,0) \quad \mathbf{r}_{2,u}(1,1) = \mathbf{r}_{3,u}(1,1)$$

are satisfied, then the blending surface $\mathbf{f}(u,v)$ *given in (2) fills the hole* G^1 *continuously. (The subscripts u and v denote the differentiation with respect to u and v, respectively.)*

Proof. According to Remark 2 the surface normals of the blending surface and the given surfaces are to be computed along the connection lines. The partial derivatives along the connection line $v = 0$ are

$$\mathbf{f}_u(u,0) = \mathbf{r}_{1,u}(u,0)$$

and

$$\mathbf{f}_v(u,0) = \cos^2(\frac{\pi}{2} \cdot u)\mathbf{r}_{1,v}(u,0) + \sin^2(\frac{\pi}{2} \cdot u)\mathbf{r}_{3,v}(u,0).$$

Since $\mathbf{r}_{1,v}(u,0)$ and $\mathbf{r}_{3,v}(u,0)$ are by assumption parallel, the surface normals of $\mathbf{f}(u,v)$ and $\mathbf{r}_1(u,v)$ are also parallel along the connection line $0 < u \le 1$. The continuity between $\mathbf{f}(u,v)$ and $\mathbf{r}_2(u,v)$ along the border line $v = 1$ of the hole can be checked in a similar way.

The partial derivatives along the connection line $u = 1$ due to the conditions on the derivatives are

$$\mathbf{f}_u(1,v) = \mathbf{r}_{3,u}(1,v)$$

and

$$\mathbf{f}_v(1,v) = \mathbf{r}_{3,v}(1,v),$$

which result the G^1 continuity of the two surfaces.

At the singular point $u = 0$ two cases can be differentiated. If one of the surfaces $\mathbf{r}_1(u,v)$ and $\mathbf{r}_2(u,v)$ has no tangent plane or they have different tangent planes at the singular point then the resulting surface has no tangent plane at this point either.

If the point $u = 0$ of the surfaces $\mathbf{r}_1(u,v)$ and $\mathbf{r}_2(u,v)$ is singular only in the parametrization, then the unit vector of the surface normal at the singular point can be defined as $\lim_{u\to0}(\mathbf{r}_{1,u}(u,v_0) \times \mathbf{r}_{1,v}(u,v_0))^0$ and $\lim_{u\to0}(\mathbf{r}_{2,u}(u,v_0) \times \mathbf{r}_{2,v}(u,v_0))^0$, respectively, where $v_0 \in [0,1]$ and the 0 in the exponent denotes the normalization of the vectors. This definition of the surface normal at singular points has been applied also by Reif (1995). By assumption, the two surfaces have a common tangent plane at the corner point of the hole, consequently these two vectors are equal to the

common surface normal denoted by **n**. We show that the resulting surface $\mathbf{f}(u,v)$ has the same tangent plane at this point (Fig. 10). Namely,

$$
\begin{aligned}
\lim_{u\to 0}\mathbf{f}_u(u,v_0) &= \cos^2(\frac{\pi}{2}v_0)\cdot \lim_{u\to 0}\mathbf{r}_{1,u}(u,v_0) \\
&+ \sin^2(\frac{\pi}{2}v_0)\cdot \lim_{u\to 0}\mathbf{r}_{2,u}(u,v_0)
\end{aligned}
$$

and similarly

$$
\begin{aligned}
\lim_{u\to 0}\mathbf{f}_v(u,v_0) &= \cos^2(\frac{\pi}{2}v_0)\cdot \lim_{u\to 0}\mathbf{r}_{1,v}(u,v_0) \\
&+ \sin^2(\frac{\pi}{2}v_0)\cdot \lim_{u\to 0}\mathbf{r}_{2,v}(u,v_0), \quad v_0\in[0,1].
\end{aligned}
$$

Moving along a $v = v_0$ parameter line into the singular point, the surface normal defined as $\lim_{u\to 0}(\mathbf{f}_u(u,v_0)\times \mathbf{f}_v(u,v_0))^0$ is also parallel to **n**, because all the vector components in this expression are perpendicular to **n**. Consequently, the constructed blending surface $\mathbf{f}(u,v)$ has the same tangent plane at $(u,v) = (0,0)$ as the surfaces $\mathbf{r}_1(u,v)$ and $\mathbf{r}_2(u,v)$. ⋄

In Fig. 8 the three-sided surfaces are ellipsoids and the third one is a cylindrical surface. The drawn parts are parametrized as follows. $\mathbf{r}_1(u,v)$: $(u,v)\in[0,1]\times[-1,0]$; $\mathbf{r}_2(u,v)$: $(u,v)\in[0,1]\times[1,2]$; $\mathbf{r}_3(u,v)$: $(u,v)\in[1,3]\times[0,1]$.

The example in Fig. 10. illustrates the G^1 continuous filling of the three-sided hole shown in Fig. 8. Fig. 9 shows the surface patches used in equation (2).

Similar modelling problems occur e.g. in planning a roof by joining a conic and a planar part smoothly around a corner, while also matching a third surface (a part of a wall or eaves).
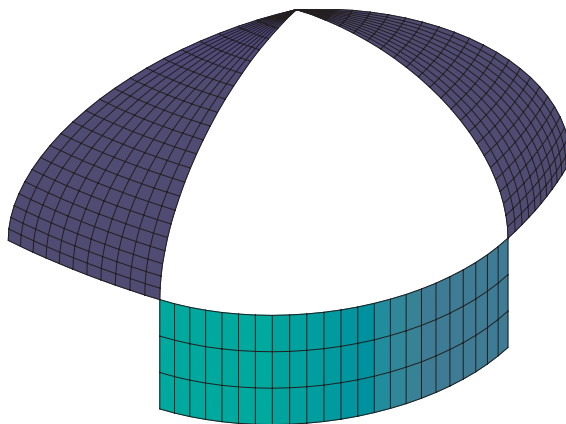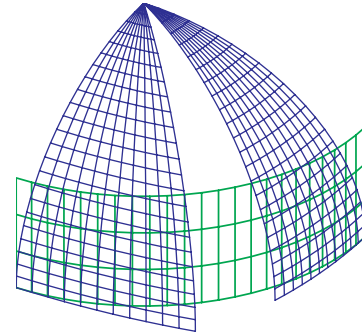

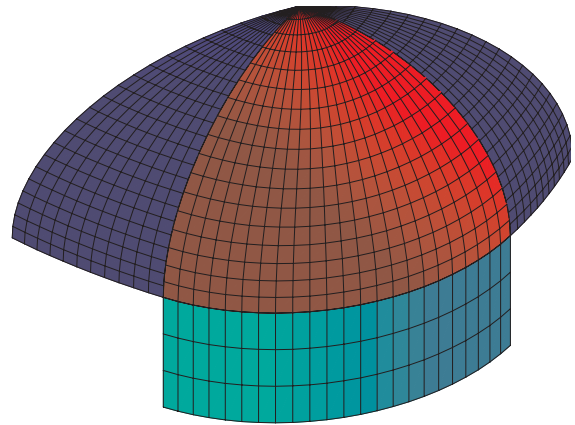Figure 9: The combined surface pieces.

Figure 10:Filling the hole shown in Fig. 8.

4   Rational parametrization of the trigonometrical blending functions

In the algorithms shown in Sections 2 and 3 there are no restrictions on the type of the parametric vector functions describing the surfaces bordering the gap or the hole. However, the implementations in the praxis usually work with polynomial or rational spline functions. Consequently, when the curves and surfaces are described by rational functions, the blending functions in the convex combination should be also given in polynomial or rational form. Based on the rational parametrization of the circle and fundamental identities the trigonometric blending functions in (1) and (2) can be replaced as follows. Choosing the function

$$
\mu(t) = \frac{4t^2}{(1+t^2)^2}, \quad 0\le t\le 1,
$$

the substitutions

$$
\sin^2(\frac{\pi}{2}\cdot t) = \mu(t) \quad \text{and} \quad \cos^2(\frac{\pi}{2}\cdot t) = 1-\mu(t) \tag{3}
$$

Figure 8: Two ellipsoids and a cylinder around the hole.

(t is standing instead of u or v) lead to an equivalent definition of the surface in (1) or in (2). The Theorems and the Remarks above yield further on, since the functions in (3) behave equally at $t = 0$ and $t = 1$. Of course, the parametrization of the resulting surface will be different. The higher numerical stability of the rational blending functions in the neighbourhood of the singular point yields smoother surfaces than the trigonometric functions. However, the investigation of the boundary values of the functions and their derivatives is more transparent in the trigonometric form.

The surfaces shown in Figs. 4, 6 and 10 are generated in this rational form. Similarly, the rational form is used in the next example of a three-sided hole. The surface on the right-hand side is a planar triangle (Fig. 11.), on the left-hand side an ellipsoide and the lower one is a cylindrical surface with a quintic Bézier generator curve. The blending surface filling the hole joins with G^1 continuity to the three given surfaces.
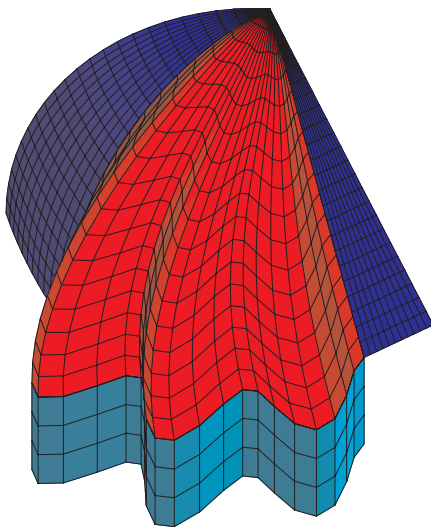

Figure 11: Filling the hole formed by an ellipsoid, a planar triangle and a cylindrical surface by rational blending.

5   Conclusions

The given methods for generating surfaces filling a gap between two surfaces or a three-sided hole are based on convex combinations of the surfaces surrounding the gap or the hole, respectively. This concept is a new approach of Coons's blending methods. The resulting surfaces fit the given surfaces along the connection curves with C^0, C^1, G^1 or C^2 continuity depending on the geometric inputs and correction functions. Both surface constructions are of importance in the practice, when traditional methods (subdivision algorithms in the first case or construction of control

points in the second case) do not work. As CAD-systems frequently use degenerate rectangular patches which cannot be handle by methods developed for triangular surfaces, our method for C^1 or G^1 filling of a three sided hole is useful in such applications.

The assumptions in the Theorems allow parameter transformations on the constituents of the convex combination. Our experiments have shown that some parameter transformations do not influence the shape of the resulting surface. This shape influence of different parametrizations and weaker continuity conditions could be the subject of further investigations.

The computations and the drawings have been made by the symbolical algebraic program package Maple V R5.

References

Alfeld, P. and Barnhill, R.E. (1984), A transfinite C^2 interpolant over triangles, Rocky Mountain Journal of Mathematics 14, 17-39.

Bär, G. (1977) Parametrische Interpolation empirischer Raumkurven. ZAMM 57, 305-314

Boehm, W. (1988) Visual continuity. Computer-aided Design 20, 307-311

Farin, G. (1990) Curves and Surfaces for Computer Aided Geometric Design, A Practical Guide. Academic Press, Inc., San Diego

Filip, D. J. (1989) Blending Parametric Surfaces. ACM Transactions on Graphics, 8, 164-173

Gregory, J.A. (1985) Interpolation to boundary data on the simplex. Computer Aided Geometric Design 2, 43-52

Gregory, J.A. (1989) Geometric continuity. In: T. Lyche and L. Schumaker eds. (1989) Mathematical methods in CAGD. Academc Press, New York, pp. 353-371

Hartmann, E. (2001) Parametric G^n blending of curves and surfaces. Visual Computer, 17, 1-13

Hoschek, J. and Lasser, D. (1992) Grundlagen der geometrischen Datenverarbeitung. 2. Aufl., B.G. Teubner, Stuttgart

Little, F.F. (1983) Convex Combination Surfaces In: R.F. Barnhill and W. Boehm eds. (1983) Surfaces in CAGD. North-Holland Publishing Company, pp. 99-107

Reif, U. (1995) A unified approach to subdivision algorithms near extraordinary vertices. Computer Aided Geometric Design 12, 153-174

Schichtel, M. (1993) G^2 Blend Surfaces and Filling of N-Sided Holes. IEEE Computer Graphics & Applications 13, 68-73

Szilvási-Nagy, M. and P.Vendel, T. (2000) Generating curves and swept surfaces by blended circles. Computer Aided Geometric Design 17, 197-206

Szilvási-Nagy, M. (2000) Konstruktion von Verbindungsflächen mittels trigonometrischer Bindefunktionen. 25. Süddeutsches Differentialgeometrie-Kolloquium den 2.6.2000, Institut für Geometrie Technische Universität Wien (to appear)

Márta Szilvási-Nagy

Dept. of Geometry

Budapest University of Technology and Economics

H-1521 Budapest, Hungary

e-mail: szilvasi@math.bme.hu

Teréz P. Vendel

Dept. of Mathematics,

University of Pécs

Boszorkány u. 2, H-7624 Pécs, Hungary

vendel@witch.pmmf.hu

Hellmuth Stachel

Inst. of Geometry

Vienna University of Technology

Wiedner Hauptstrasse 8-10, A-1040 Wien, Austria

e-mail: stachel@geometrie.tuwien.ac.at